Sakarya Üniversitesi Fen Bilimleri Dergisi
Sakarya University Journal of Science

e-ISSN : 2147-835X
Publisher : Sakarya University

Vol. 29, No. 5, 580-591, 2025
DOI: https://doi.org/10.16984/saufenbilder.1750450

Research Article

The Effects of Pre-evaporation Time on the Structure and Performance of Na-Lignosulfonate/PVA Composite Films

Emir Erişir

Sakarya University of Applied Sciences, Pamukova Vocational School, Department of Material and Material Prcessing Technologies, Sakarya, Türkiye, emirerisir@subu.edu.tr, ror.org/01shwhq58
*Corresponding Author

ARTICLE INFO

Keywords:
Sodium lignosulfonate
Lignin
Polyvinyl alcohol
Film
Solvent removal

Article History:
Received: 25.07.2025
Revised: 22.09.2025
Accepted: 23.09.2025
Online Available: 21.10.2025

ABSTRACT

Lignin, an abundant renewable biopolymer in nature, contains specific structural limitations affecting its application strategies. So, a favoured strategy is to use it into the manufacturing of composite materials with other natural or synthetic polymers. This study examines the impact of controlled accelerated solvent removal (pre-evaporation), a subject that is still not thoroughly explored, on the structural, morphological, and thermal characteristics of Na-lignosulfonate (LS) and polyvinyl alcohol (PVA) composite films. Aqueous solutions containing LS, PVA, glycerol and urea were formulated for the casting of composite films. A pre-evaporation at 85-90 °C for 0 to 240 min was employed to solution enhancing its concentration prior to being poured into moulds. The ^{13}C-NMR and FTIR used for structural characterisation validated the specific aromatic and aliphatic structure of LS. FTIR analysis identified interactions between LS and PVA in the films, indicating changes in the ether bond peaks (~1039 cm^{-1}). TGA demonstrated that LS enhanced the thermal stability of the composites and facilitated carbonisation above 450°C. Examination by SEM of the composite films indicated that the pre-evaporation duration significantly affected the morphology. A 5–14% decrease in film thickness and an increase in pore size and number, particularly on the exposed surface, were observed, but the change did not occur uniformly. LS/PVA films were effectively produced without internal stress during pre-evaporation durations of up to 150 min. At times exceeding 150 min, excessive solvent loss and increased solution viscosity resulted in significant morphological defects such as internal stresses, large pores, and structural integrity failure, leading film casting impossible at 240 min. The study determined that the 150 min pre-evaporation procedure is an essential limit for the production of composite films from these polymers. The results obtained are crucial for improving the processing parameters of lignin-based composites intended for packaging or carbon precursor applications.

1. Introduction

A considerable portion of biopolymer research focuses on biomass components, including cellulose, hemicellulose, and lignin, which are some of the most abundant polymers in nature. Lignin, a natural aromatic polymer, is a crucial structural component, providing rigidity and strength to plant cell walls, and serves as a renewable feedstock. It is found heterogeneously distributed in the middle lamella within the cell wall and between cells. However, lignin is found in the middle lamella or cell walls in a complex mixture with other plant polymers, which complicates its pure extraction and direct utilization.

The diversity of plant sources from which lignin is obtained, and delignification methods enable the production of different types of lignin suitable for various application areas. In addition to traditional lignin types such as kraft lignin and lignosulfonates, new-generation lignin variants obtained through methods such as steam

Cite as: E. Erişir, "The effects of pre-evaporation time on the structure and performance of Na-lignosulfonate/pva composite films," Sakarya University Journal of Science, vol. 29, no. 5, pp. 580-591, 2025. https://doi.org/10.16984/saufenbilder.1750450

explosion, organosolv, deep eutectic solvents, or dilute acid treatments are also available [1].
The fact that the pulping (or delignification) method directly affects the physical and chemical properties of lignin significantly expands and diversifies the application areas of this valuable biopolymer. Historically, lignin was considered a waste product, especially for the paper industry, and until recently, it was generally disposed of by burning for energy production.

In recent years, research into the use of this valuable biopolymer and its composites as carbon precursors for graphene production has attracted considerable attention [2-9]. However, the limited film-forming capabilities of lignin and its derivatives limit their direct application. Therefore, the evaluation in combination with other polymers is essential for applications such as film production.

Due to its water solubility, biodegradability potential, and compatibility with natural polymers [10, 11], polyvinyl alcohol (PVA) is a widely used polymer such as lacquers, adhesives, surface coating materials, films, and plastic materials [12]. While lignin/PVA composite films have been successfully produced, the studies investigating the effects of process parameters on film properties during film production are relatively limited in the literature.

In this study, the effects of increasing the lignin/PVA solutions concentration before the film casting process on film properties were investigated. It was anticipated that film characteristics would rise to a specific threshold with increasing concentration, subsequently declining thereafter. To this end, a controlled accelerated solvent removal process was applied to increase the concentration of solutions prepared at a specific initial concentration. The solutions obtained at different concentrations were cast into molds of the same volume and size to produce films, and the structural, thermal and morphological properties of these films were thoroughly investigated.

2. General Methods

2.1. Materials

Sodium lignosulfonate (LS, Pars Kimya, M_w: 500-2000 g/mol), polyvinyl alcohol (PVA, Merck, ≥98% hydrolzed, M_w: 60000 g/mol), glycerol (Balmumcu Kimya, USP grade, M_w: 92.09 g/mol), and urea (Merck, M_w: 60.06 g/mol, purity ≥99%) were used for film production without any purification procedure. Deionized water (DI) was utilized throughout all production and characterization phases.

2.2. Production of lignin-PVA films

Approximately 2.00 g of PVA was dissolved in 20 ml of DI water. The dissolution was conducted in an oil bath at 85-90°C, with magnetic stirring maintained at a constant speed of 500 rpm. In another container, approximately 2.00 g of LS, 0.20 g of urea, and 4.00 ml of a 25 wt% glycerol solution were dissolved in 20 ml of DI water using a stirring rod. The solution was thereafter allowed to heat at 85-90°C. After 15 min, the LS solution (20 ml) was incorporated into the PVA solution (20 ml). The container was covered and the LS-PVA mixture was continued to be stirred at 85–90°C and 500 rpm for 60 min. At the end of the 60 min mixing period, the cover of the reaction container was removed to facilitate the preliminary evaporation of the solvent. The preliminary evaporation of water occurred for 0, 30, 60, 90, 105, 120, 135, 150, 180 or 240 min.

The prepared LS-PVA mixture was poured into two silicon casting molds with an inner diameter of 10 cm and allowed to cure at 28°C for approximately 12-16 hours in a climate-controlled setting. Upon completion of the drying period, the films were removed from the molds and preserved in zip-sealed bags.

2.3. Characterization methods

2.3.1. Wet chemistry analysis

The lignin and ash contents of sodium lignosulfonate were determined according to TAPPI standards (T222 om-11 and T211 om-02, respectively).

2.3.2. NMR analysis

NMR studies were performed to evaluate the structure of LS. Samples were dissolved to make 20 g/L solutions in DMSO-d_6 for analysis on a Bruker Ascend high-resolution digital 500 MHz nuclear magnetic resonance (NMR) spectrometer.

2.3.3. Thermogravimetric (TGA) analysis

A Mettler Toledo TGA 2 model thermogravimetric analyser was used for thermal analysis. Approximately 8.00 mg of sample was accurately weighed for each test. The tests were conducted under a nitrogen atmosphere at a heating rate of 10°C/min within a temperature range of 30°C to 900°C.

2.3.4. Fourier transform infrared spectroscopy

A Bruker Optik GMBH Tensor 37 instrument was used for the measurements. Operating range was from 4000 to 400 cm^{-1} and the spectral resolution was set to 2 cm^{-1}.

2.3.5. Scanning Electron Microscopy (SEM)

Images from a scanning electron microscope (SEM) were obtained to analyze the morphological properties of the films. The images were captured from both surfaces of the films: the open (exposed) surface where evaporation occurred unimpeded and the closed surface in contact with the mold. Prior to starting the imaging process, the films were cut into small pieces for the morphological imaging. The samples were subsequently coated with gold-palladium before measurement. Imaging was conducted utilizing a Thermo Scientific Axia device at magnification levels of 100x, 1000x, 2500x, and 5000x. All tests were performed under vacuum conditions at an acceleration voltage of 15 kV.

3. Results and Discussion

3.1. Characterization of neat lignosulfonate

The structural characteristics of LS obtained commercially from a local provider were determined using wet chemical and instrumental analysis methods. The lignin content of LS was determined to be 93.92%, while the ash content was found to be 5.86%. The spectrum obtained from the ^{13}C-NMR analysis is presented in Figure 1.

The aliphatic carboxyl groups in LS were observed at 172.54 ppm [13-15]. The absence of distinct signals in the 90–102 ppm range indicates that the sample contains a low amount of residual wooden carbohydrates [15]. In the 161.43–112.33 ppm range, aromatic moieties of lignin were detected in accordance with previous studies [14, 16-18]. In this region, strong signals indicating p-coumaric ester for C-4 were identified around 159 ppm [15], while similarly strong signals for aromatic C–H of C5 were present between 114.63 and 116.93 ppm [18].

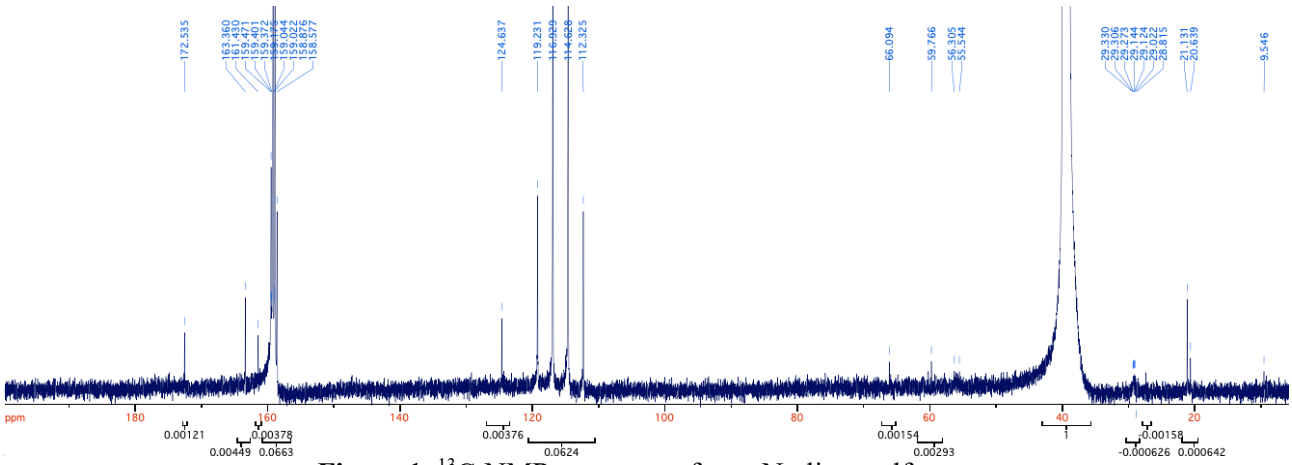

Figure 1. ^{13}C-NMR spectrum of neat Na-lignosulfonate

Relatively weaker signals observed at 112.33 and 119.23 ppm indicate aromatic C–H bonds in C2 and C6, respectively [18]. Aliphatic oxygen-containing groups are present in the 60–90 ppm region [19]. The signals indicating the carbon in the methoxy group were detected at 56.31 ppm [13-14, 18]. The strong signal in the 40 ppm region is attributed to DMSO-d6, which was used to dissolve the sample.

The FTIR patterns of neat LS in Figure 2 reveal that peaks associated with C=C stretching vibrations from the aromatic ring structure of the lignin, detected at 1440–1594 cm^{-1} [18, 20-22].

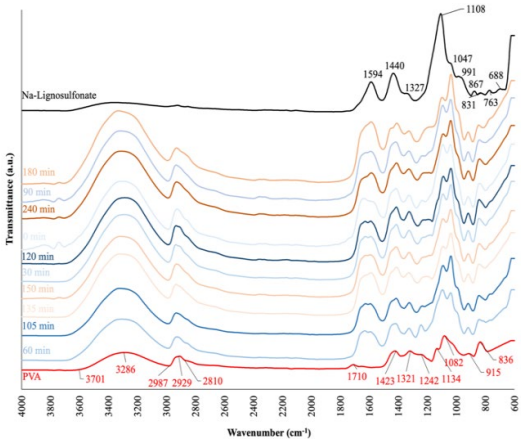

Figure 2. The FTIR spectrum of neat PVA and LS with their films

Very weak absorptions indicating methylene and methyl groups of side chains and aromatic methoxy groups were observed in the 2800–3000 cm^{-1} range, and hydroxyl groups were indicated in the 3000–3600 cm^{-1} range [23]. A shoulder at 1047 cm^{-1} indicates S=O stretching and sulfonate group (SO_3) absorption vibrations [18, 20-21].

The vibrations observed in the 900–750 cm^{-1} region are attributed to bending vibrations from aromatic component C-H bonds, and the vibrations observed in the 1280–1030 cm^{-1} region are attributed to stretching vibrations from C-O bonds of various alcohols, phenols, esters, and ethers [24]. The vibration observed around 688 cm^{-1} is thought to originate from the out-of-plane bending of C–H bonds [18].

3.2. Characterization of lignosulfonate-PVA films

3.2.1. FTIR analysis

The FTIR pattern of neat PVA presented in Figure 2 exhibits some characteristic bands. The PVA skeletal band was observed at 836 cm^{-1} [25]. In the 3000-3600 cm^{-1} region, stretching vibrations indicating O–H from intermolecular and intramolecular hydrogen bonds can be clearly observed compared to the LS pattern [26]. However, the magnitude of this peak is small rather than that of LS-PVA films, as explained later. Furthermore, the bending vibration of OH groups can be seen in the 1423-1242 cm^{-1} band range [27].

In the same figure, the stretching vibration of C–H from alkyl groups was detected in the 2810–2927 cm^{-1} band range [28, 29] while C-O stretching vibrations were observed around 1134 cm^{-1} [27, 29]. Additionally, the vibrational band in this region is attributed to the crystallinity of PVA [26]. Weak shoulders observed in the 1000–1200 cm^{-1} band range were detected at 1082 cm^{-1} in this study and are attributed to ether bonds [30]. The vibrations observed in the form of shoulders at 1710 cm^{-1} are attributed to stretching vibrations originating from C=O [29].

Upon comparing the FTIR spectra of LS-PVA films, it was observed that the peak intensity corresponding to OH groups, which are indicative of neat LS and PVA, increased in the 3000–3600 cm^{-1} range. In contrast, according to Su & Fang [27], the vibration peaks in the relevant region decreased compared to neat polymers. A possible explanation for this is that water evaporation without a thermal process was carried out during film formation, resulting in a large amount of remaining water in the film.

The peak observed at 1030 cm^{-1} has been identified by previous researchers as indicating an ether bond (C-O-C), and it has been determined that the magnitude of this peak is related to the extent of the aldol reaction between lignin and PVA [31]. In the present study, the relevant peak was observed at 1039 cm^{-1}, but it is slightly affected by the peak at 1108 cm^{-1}, which belongs to the stretching vibrations of the C-O functional groups of LS. However, the same peak was observed with a shift to 1097 cm^{-1}, and its intensity decreased. Additionally, the sulfur-containing compounds present in LS also vibrate in a region very close to this point. As a result of these interactions, both a slight change in peak intensity and a slight shift in the expected wavenumber have occurred. However, despite all

this, it is clear that there is an interaction between LS and PVA.

3.2.2. TGA and DTG analysis

The effects of different pre-evaporation times (0–240 min) on the thermal behaviour of LS/PVA films derived from solutions were investigated using TGA and DTG curves presented in Figures 3 and 4.

In the initial analysis of the TGA curves (Figure 3), common trends were identified. A multi-step and gradual thermal degradation was observed in both neat PVA and all LS/PVA films between 30°C and 900°C. A distinct mass loss starting at 30°C and ending around 120°C was also observed in all samples, which is generally associated with the removal of free and bound water from the polymers [32, 33]. DTG curves (Figure 4) also show peaks of varying sizes in this region. Notably, neat PVA demonstrates the lowest mass loss compared to other samples in this specific region, which is consistent with the FTIR patterns presented in Figure 2.

The mass loss of neat PVA accelerated around 300°C, reached 50% at about 350°C and 90% around 430°C. The complete decomposition of PVA mass observed at approximately 494°C. All these stages were reported in previous studies describing the degradation and dehydrogenation of the PVA main chain [33]. In films containing lignosulfonate, it was observed that at least 30% of the mass was retained at the temperature at which PVA was completely degraded.

The degradation of LS/PVA composite films follows a three-stage process (Figures 3 and 4). The initial region, beginning around 180°C and extending to approximately 250°C, indicates certain reactions resembling, yet occurring at lower temperatures compared to, the degradation process of neat PVA. The DTG curves (Figure 4) distinctly exhibit peaks associated with these modifications. It is hypothesized that the main degradation mechanism of PVA is affected and occurs at lower temperatures due to the degradation of low molecular weight and unstable lignosulfonate components and side chains attached to the aromatic ring of lignin in this region [34].

The more stable aromatic structure and higher molecular weight components of lignosulfonate degrade at higher temperatures compared to the lower molecular weight lignin chains. Given that neat PVA is expected to completely degrade above 450°C, the significant amount of residual mass detected above this temperature in LS/PVA films is explained by their char formation tendency [34].

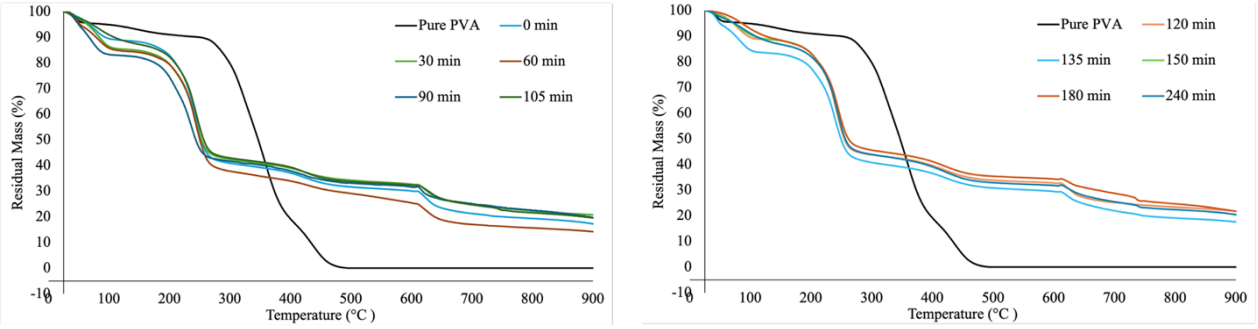

Figure 3. Thermal decomposition graphs of neat PVA and LS/PVA films

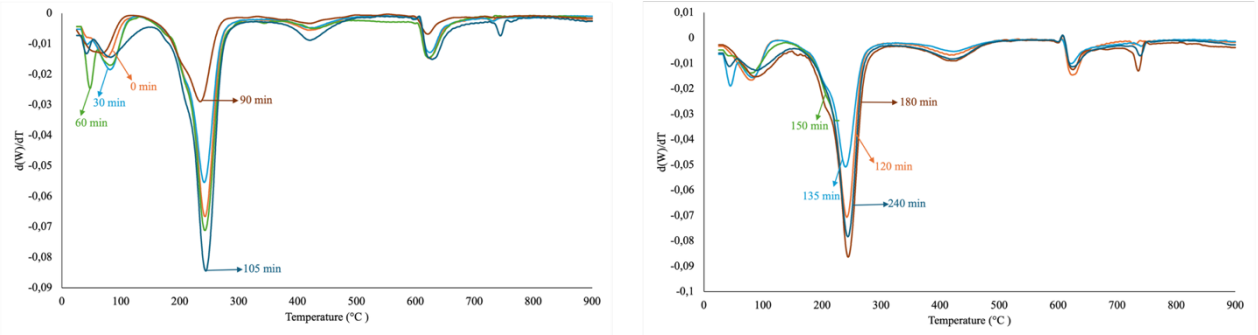

Figure 4. DTG curves for LS/PVA films

The thermal decomposition results suggest that the stepwise degradation observed in LS/PVA films holds promise for graphene production without the need for a substrate. Extensive research on this topic is planned for subsequent studies.

3.2.3. SEM analysis

The morphological structures of the films were examined using SEM with the previously described method and the film images were presented in Figures 5 and 6. This enabled a topographical comparison between the open (top) surfaces (contact with atmosphere) and the closed (bottom or mold-contacting) surfaces (contact with the filming mold) of films.

Increasing the pre-evaporation time during film formation caused significant structural changes in the morphology and surfaces of films. The most critical effect observed was the evolution of porosity. As the pre-evaporation time extended from 150 to 240 min, the increased solvent removal led to a higher viscosity of the lignin-PVA solution. This led to disorders in the film matrix and the larger pores.

It was found that the film-forming ability of the samples cast from solutions applied above 150 min of pre-vaporization is significantly reduced. The situation can be clearly recognized from the macroscopic images of the films depicted in Figures 7. This phenomenon can be attributed to the increase in viscosity of solution resulting from the evaporation of more than half of the solvent, leading to the formation of a thicker, gel-like matrix. The gelation prevents the solution from spreading uniformly in the mold, inhibiting the formation of a continuous, smooth film layer. Changing the evaporation rate is known to raise the internal tension during high film development [35]. Conversely, the research by Feng et al. [36] revealed that films produced from higher concentration solutions had superior surface morphology.

Extended pre-vaporization reduced the drying time, but it probably increased internal stresses, leading to the deterioration of film morphology. Excessive solvent loss makes it difficult for polymer chains to rearrange and form a stable network structure, leading to microstructural defects, which in turn reduce the integrity and morphological quality of the films.

SEM images of the films with higher magnifications such as 2500 and 5000x revealed a network structure morphology as a network structure up to 150 min. However, this network structure appears to be layered, especially for some films. A noticeable colour difference can be observed between the closed and open surfaces of the films. The bottom surfaces that encounter the mold surface of the films take on a distinct light color, while the upper surfaces are darker in tone (Figure 7).

The chemical incompatibility between lignosulfonate and PVA can be seen in film morphology as polymer aggregates and microphase separation [37]. It was shown that at elevated lignin concentrations, additional lignin does not interact uniformly with the PVA matrix, functioning just as a filler [38]. This results in a heterogeneous morphology that decreases the film's structural integrity and adversely affects its mechanical properties. This kind of behaviour is quite similar to the idea of microphase separation, which describes how two parts of a film might generate separate phases at the molecular level

4. Conclusion

This study investigated the effects of pre-evaporation time on the properties of Na-lignosulfonate (LS)/PVA composite films, identifying a critical processing threshold for successful film fabrication.

Structural characterization analyses revealed the high purity of the lignin used in the study and the details of its aromatic structure. FTIR spectroscopy indicated the characteristic vibrations of both neat LS and PVA. The presence of an ether bond vibrations around 1039 cm^{-1}, indicating aldol reactions between LS and PVA, demonstrates the successful production of composite films. However, in the films, the peaks located at 3000-3600 cm^{-1} were larger than those of both polymers, suggesting that the drying conditions chosen for film production were insufficient for solvent removal.

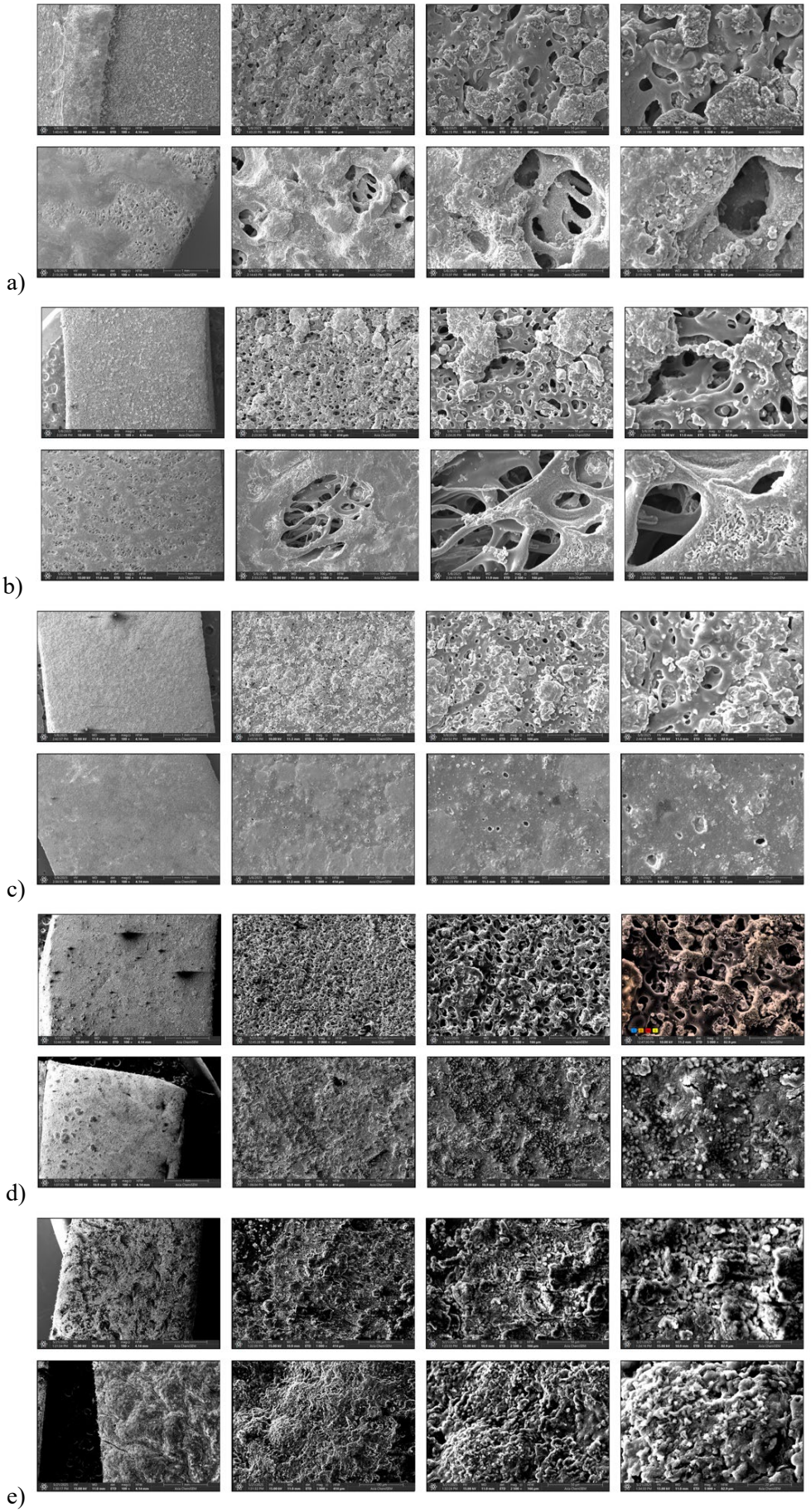

Figure 5. SEM images of lignin-PVA films' surfaces recorded at magnifications of 100, 1000, 2500, and 5000x (a: 0 min., b: 30 min., c: 60 min., d: 90 min., e: 105 min.)

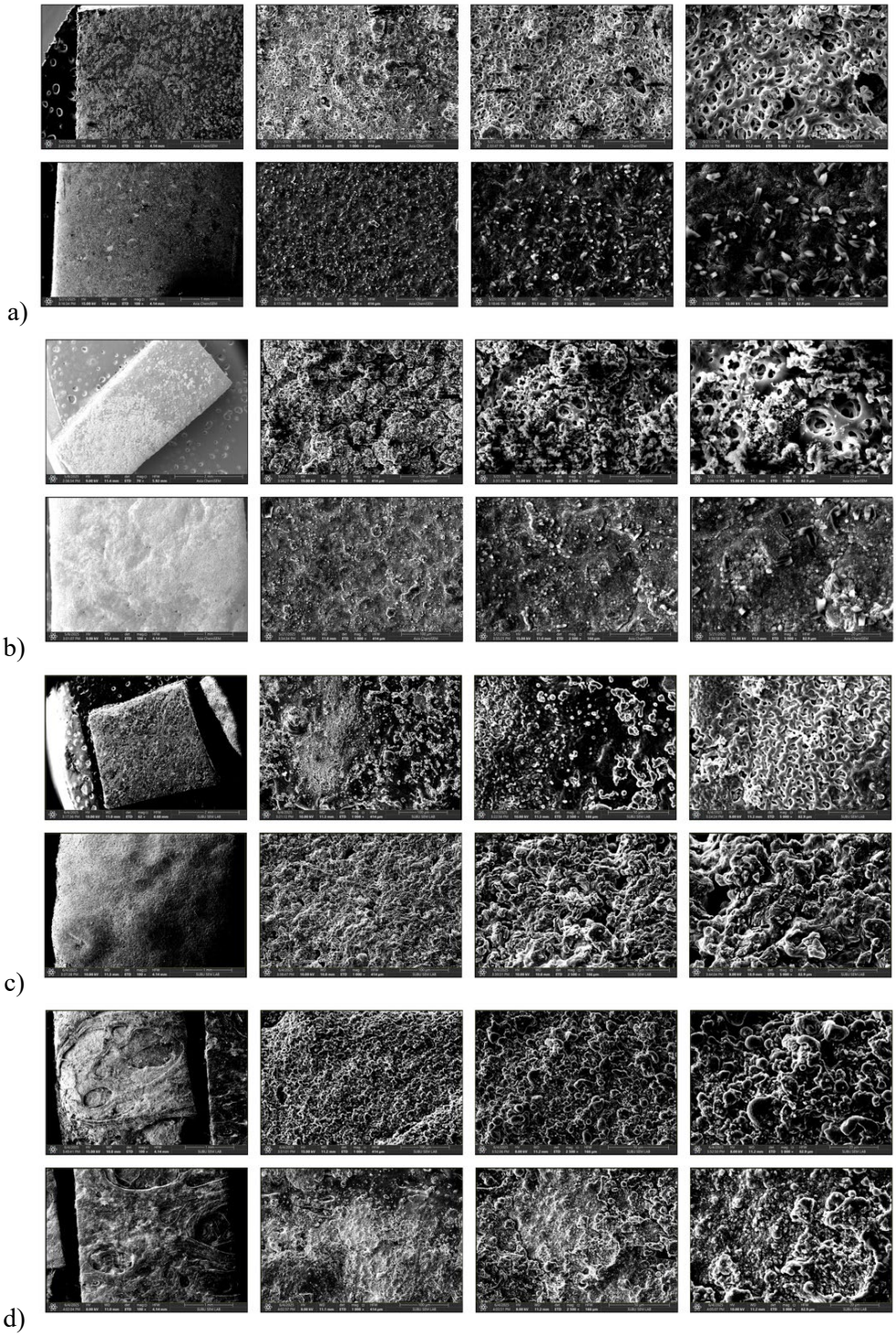

Figure 6. SEM images of lignin-PVA films' surfaces recorded at magnifications of 100, 1000, 2500, and 5000x (a: 120 min., b: 135 min., c: 150 min., and d: 240 min.)

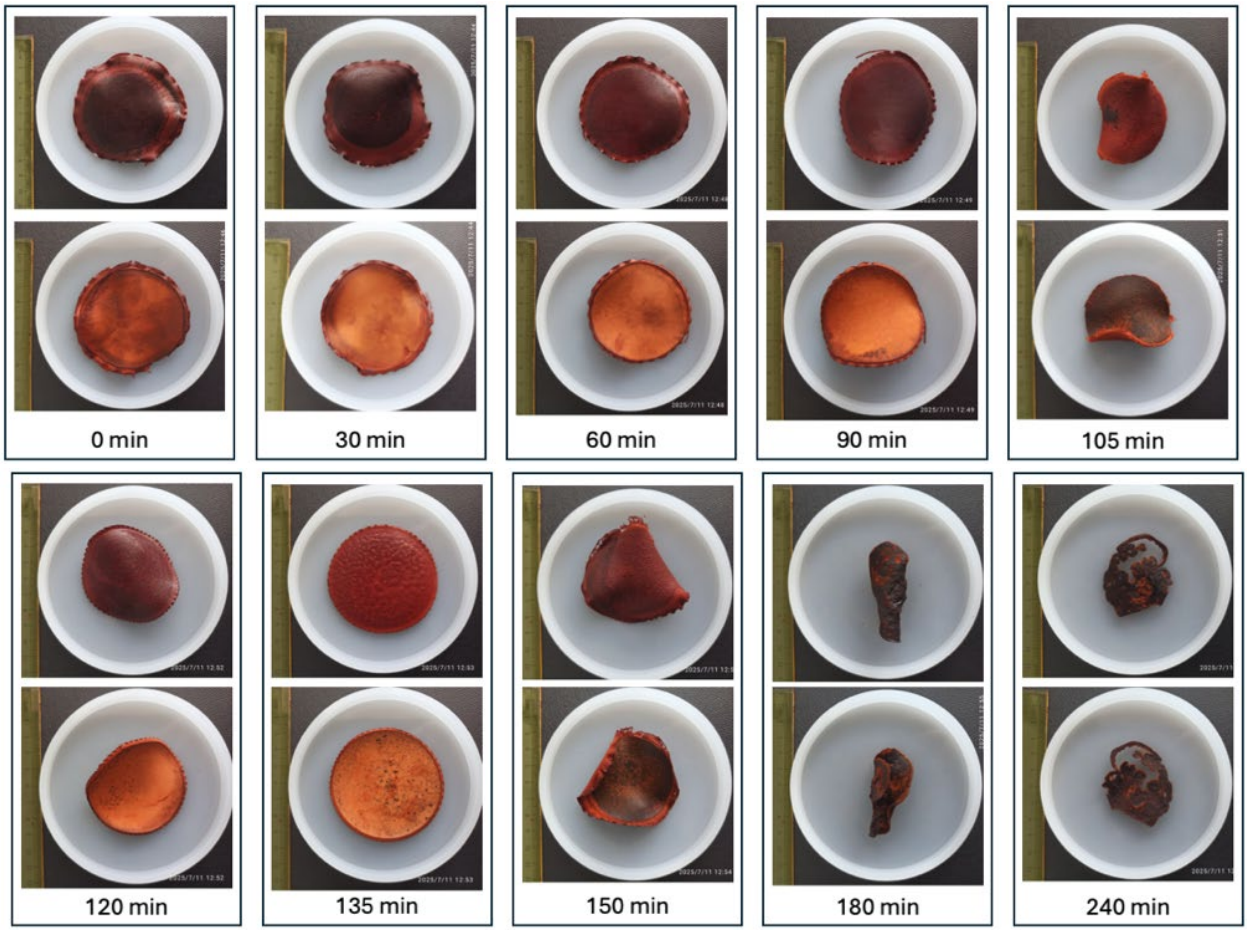

Figure 7. Macroscopic images of lignin-PVA films

A thermal treatment step at a higher temperature is needed to reduce the water content in the films. The remaining water content in the films was confirmed by thermogravimetric analysis. The most significant conclusion is the influence of pre-evaporation time on film morphology. A distinct point was found at 150 min. The pre-evaporation process created films with a continuous network structure. The process successfully increased the solution concentration without causing catastrophic consequences. Prolonged pre-evaporation led to the removal of excessive amounts of solvent, creating a highly viscous, gel-like solution. It resulted in a solution that was not spread evenly across the mold, creating a lot of internal stress in the film.

Thermogravimetric investigations demonstrated that the addition of LS enhanced the thermal stability of neat PVA and promoted carbonisation in the composites at elevated temperatures (>450°C). This, along with the mentioned enhancements in film structure, increases the possible uses of these composites for applications requiring heat resistance or as precursors to carbon-based materials like graphene.

Consequently, the pre-evaporation process must be carried out with considerable precision. It saves time by removing excess solvent from the casting solution, but the time must be carefully optimized within a narrow range (≤150 min under these specific conditions) to avoid morphological defects. Future research should focus on removing residual solvent from the films and exploring opportunities for improvement in interfacial adhesion and microphase separation.

Article Information Form

Acknowledgments

The author would like to sincerely thank Mert Kaban (Sakarya University of Applied Sciences) for performing the SEM imaging and Rumeysa Yildirim (Kocaeli University) for her assistance with tensile testing experiments. In addition, the author gratefully acknowledges the Department of Metallurgical and Materials Engineering at

Kocaeli University for providing access to their laboratory facilities.

The Declaration of Conflict of Interest/ Common Interest

No conflict of interest or common interest has been declared by the author.

Artificial Intelligence Statement

No artificial intelligence tools were used while writing this article.

Copyright Statement

References

[1] H. Chung, N. R. Washburn, "Extraction and types of lignin," in Lignin in Polymer Composites, O. Faruk and M. Sain, Eds. Oxford, UK: Elsevier Inc., pp. 13-25, 2016.

[2] Y. Lei, A. H. Alshareef, W. Zhao, S. Inal, "Laser-scribed graphene electrodes derived from lignin for biochemical sensing," ACS Applied Nano Materials, vol. 3, no. 2, pp. 1166-1174, 2020.

[3] Y. Lei, W. Zhao, Y. Zhu, U. Buttner, X. Dong, H. N. Alshareef, "Three-dimensional Ti_3C_2T x MXene-Prussian blue hybrid microsupercapacitors by water lift-off lithography," ACS Nano, vol. 16, no. 2, pp. 1974-1985, 2022.

[4] C. Lee, S. Jeong, Y. Kwon, J. Lee, S. Cho, B. Shin, "Fabrication of laser-induced graphene-based multifunctional sensing platform for sweat ion and human motion monitoring," Sensors and Actuators A: Physical, vol. 334, p. 113320, 2021.

[5] Y. Lin, Q. Zhang, Y. Deng, Q. Wu, X. P. Ye, S. Wang, G. Fang, "Fabricating graphene and nanodiamonds from lignin by femtosecond laser irradiation," ACS Omega, vol. 6, no. 49, pp. 33995-34002, 2021.

[6] F. Mahmood, C. Zhang, Y. Xie, D. Stalla, J. Lin, C. Wan, "Transforming lignin into porous graphene via direct laser writing for solid-state supercapacitors," RSC Advances, vol. 9, pp. 22713-22720, 2019.

[7] L. Meng, S. Chirtes, X. Liu, M. Eriksson, W. C. Mak, "A green route for lignin-derived graphene electrodes: A disposable platform for electrochemical biosensors," Biosensors and Bioelectronics, vol. 218, p. 114742, 2022.

[8] K. Sinha, L. Meng, Q. Xu, X. Wang, "Laser induction of graphene onto lignin-upgraded flexible polymer matrix," Materials Letters, vol. 286, p. 129268, 2021.

[9] A. Wen, C. Wang, J. Nong, C. Hu, "Rapid construction of robust and hydrophilic lignin-derived laser-induced graphene electrodes using PVA-free dopants," Carbon, vol. 232, p. 119767, 2025.

[10] J. Du, J. Guo, Q. Zhu, J. Guo, J. Gu, Y. Wu, L. Ren, S. Yang, J. Jiang, "Enhancement of polyvinyl alcohol-based films by chemically modified lignocellulosic nanofibers derived from bamboo shoot shells," Polymers, vol. 17, no. 11, p. 1571, 2025.

[11] S. G. Jin, "Production and application of biomaterials based on polyvinyl alcohol (PVA) as wound dressing," Chemistry–An Asian Journal, vol. 17, no. 21, p. e202200595, 2022.

[12] R. Nagarkar, J. Patel, "Polyvinyl alcohol: A comprehensive study," Acta Scientific Pharmaceutical Sciences, vol. 3, no. 4, pp. 34-44, 2019.

[13] R. El Hage, N. Brosse, L. Chrusciel, C. Sanchez, P. Sannigrahi, A. Ragauskas, "Characterization of milled wood lignin and ethanol organosolv lignin from miscanthus," Polymer Degradation and Stability, vol. 94, no. 10, pp. 1632-1638, 2009.

[14] I. Korbag, S. Mohamed Saleh, "Studies on the formation of intermolecular interactions and structural characterization of polyvinyl alcohol/lignin film," International Journal of Environmental Studies, vol. 73, no. 2, pp. 226-235, 2016.

[15] L. Yang, D. Wang, D. Zhou, Y. Zhang, T. Yang, "Isolation and further structural characterization of lignins from the valonea of Quercus variabilis," International Journal of Biological Macromolecules, vol. 97, pp. 164-172, 2017.

[16] Z. Xia, L. G. Akim, D. S. Argyropoulos, "Quantitative ^{13}C NMR analysis of lignins with internal standards," Journal of Agricultural and Food Chemistry, vol. 49, no. 8, pp. 3573-3578, 2001.

[17] P. Phansamarng, A. Bacchus, F. H. Pour, C. Kongvarhodom, P. Fatehi, "Cationic lignin incorporated polyvinyl alcohol films for packaging applications," Industrial Crops and Products, vol. 221, p. 119217, 2024.

[18] S. M. Nasef, A. Sayed, G. A. Mahmoud, "Comparative study of lignin and sodium lignosulfonate extracted from irradiated and non-irradiated sawdust wastes," Radiation Physics and Chemistry, vol. 214, p. 111302, 2024.

[19] O. Y. Abdelaziz, S. Meier, J. Prothmann, C. Turner, A. Riisager, C. P. Hulteberg, "Oxidative depolymerisation of lignosulphonate lignin into low-molecular-weight products with Cu–Mn/δ-Al_2O_3," Topics in Catalysis, vol. 62, pp. 639-648, 2019.

[20] N. S. Abdelrahman, E. Galiwango, A. H. Al-Marzouqi, E. Mahmoud, "Sodium lignosulfonate: A renewable corrosion inhibitor extracted from lignocellulosic waste," Biomass Conversion and Biorefinery, vol. 14, no. 6, pp. 7531-7541, 2024.

[21] J. Ou, J. Zhao, "Modification of sodium lignosulfonate and evaluation of its potential use as detergent builders," Journal of Wood Chemistry and Technology, vol. 37, no. 2, pp. 99-109, 2017.

[22] E. S. Wibowo, B. D. Park, "Chemical and thermal characteristics of ion-exchanged lignosulfonate," Molecules, vol. 28, no. 6, p. 2755, 2023.

[23] X. Li, Y. Liu, X. Ren, "Transparent and ultra-tough PVA/alkaline lignin films with UV shielding and antibacterial functions," International Journal of Biological Macromolecules, vol. 216, pp. 86-94, 2022.

[24] E. Apaydın Varol, Ü. Mutlu, "TGA-FTIR analysis of biomass samples based on the thermal decomposition behavior of hemicellulose, cellulose, and lignin," Energies, vol. 16, no. 9, p. 3674, 2023.

[25] H. E. Mahmud, A. Kassim, Z. Zainal, W. M. M. Yunus, "Fourier transform infrared study of polypyrrole–poly (vinyl alcohol) conducting polymer composite films: evidence of film formation and characterization," Journal of Applied Polymer Science, vol. 100, no. 5, pp. 4107-4113, 2006.

[26] H. S. Mansur, R. L. Oréfice, A. A. Mansur, "Characterization of poly (vinyl alcohol)/poly (ethylene glycol) hydrogels and PVA-derived hybrids by small-angle X-ray scattering and FTIR spectroscopy," Polymer, vol. 45, no. 21, pp. 7193-7202, 2004.

[27] L. Su, G. Fang, "Characterization of cross-linked alkaline lignin/poly (vinyl alcohol) film with a formaldehyde cross-linker," BioResources, vol. 9, no. 3, pp. 4477-4488, 2014.

[28] P. B. Bhargav, V. M. Mohan, A. K. Sharma, V. N. Rao, "Structural, electrical and optical characterization of pure and doped poly (vinyl alcohol)(PVA) polymer

electrolyte films," International Journal of Polymeric Materials and Polymeric Biomaterials, vol. 56, no. 6, pp. 579-591, 2007.

[29] H. S. Mansur, C. M. Sadahira, A. N. Souza, A. A. Mansur, "FTIR spectroscopy characterization of poly (vinyl alcohol) hydrogel with different hydrolysis degree and chemically crosslinked with glutaraldehyde," Materials Science and Engineering: C, vol. 28, no. 4, pp. 539-548, 2008.

[30] S. Akhter, K. Allan, D. Buchanan, J. A. Cook, A. Campion, J. M. White, "XPS and IR study of X-ray induced degradation of PVA polymer film," Applied Surface Science, vol. 35, no. 2, pp. 241-258, 1988.

[31] L. Su, Z. Xing, D. Wang, G. Xu, S. Ren, G. Fang, "Mechanical properties research and structural characterization of alkali lignin/poly (vinyl alcohol) reaction films," BioResources, vol. 8, no. 3, pp. 3532-3543, 2013.

[32] M. E. El Moustaqim, A. El Kaihal, M. El Marouani, S. Menlayakhaf, M. Taibi, S. Sebbahi, S. El Hajjaji, F. Kifani-Sahban, "Thermal and thermomechanical analyses of lignin," Sustainable Chemistry and Pharmacy, vol. 9, pp. 63-68, 2018.

[33] M. T. Taghizadeh, N. Yeganeh, M. Rezaei, "The investigation of thermal decomposition pathway and products of poly (vinyl alcohol) by TG-FTIR," Journal of Applied Polymer Science, vol. 132, no. 25, p. 42117, 2015.

[34] Y. W. Chua, H. Wu, Y. Yu, "Interactions between low-and high-molecular-weight portions of lignin during fast pyrolysis at low temperatures," Energy & Fuels, vol. 33, no. 11, pp. 11173-11180, 2019.

[35] J. Li, M. H. P. de Heer Kloots, G. van Ewijk, D. J. van Dijken, W. M. de Vos, J. van der Gucht, "Evaporation-induced polyelectrolyte complexation: The role of base volatility and cosolvents," Langmuir, vol. 40, no. 5, pp. 2531-2542, 2024.

[36] S. Feng, D. Ma, Y. Qiu, L. Duan, "Deep insights into the viscosity of small molecular solutions for organic light-emitting diodes," RSC Advances, vol. 8, no. 8, pp. 4153-4161, 2018.

[37] G. Xu, S. Ren, D. Wang, L. Su, G. Fang, "Fabrication and properties of alkaline lignin/poly (vinyl alcohol) blend membranes," BioResources, vol. 8, no. 2, pp. 2510-2520, 2013.

[38] S. Kubo, J. F. Kadla, "The formation of strong intermolecular interactions in immiscible blends of poly(vinyl alcohol) (PVA) and lignin," Biomacromolecules, vol. 4, no. 3, pp. 561-567, 2003.